

# Creep can strengthen Clay: A Matter of Long-term Slope Stability

Roland Pusch<sup>\*1,2</sup>, Sven Knutsson<sup>1</sup>, Xiaodong Liu<sup>2</sup> and Ting Yang<sup>1,2</sup>

## Abstract

The matter of long-term stability of long, natural slopes in illitic clay is of great practical importance in Scandinavia and Canada and has been frequently discussed among geotechnical specialists. A remaining question is how such natural slopes can have remained stable, yet undergoing large strain, for hundreds and thousands of years, during which critical conditions have repeatedly occurred with calculated safety factors lower than or equal to unity according to common stability calculations based on plastic theory. The reason for this may be the role of creep shear strain that causes redistribution of stress and earth pressure leading to a state of equilibrium that is very sensitive to disturbance and represents a condition of near-failure. Triggering of occasional slides can be explained by temporary high porewater pressure caused by periods of intense rain, disturbance by pile driving, or loading by road construction etc, taken place in slopes that have been stable for very long periods of time. The mechanisms by which creep can lead to stable conditions of very old clay slopes can have the form of successive relative particle movements into a state where the interparticle bonds become stronger but of brittle character, according to a model based on stochastic mechanics.

**Keywords:** Creep, Slope stability, Stochastic mechanics, Strain

## 1 Introduction

As pointed out by Bernander [1] and others, conventional analysis of “ideal-plastic slope failure” in soft clay implies that deformations within and outside the studied soil volume are disregarded, while they are in fact determinants of the progressive failure that is often observed in nature. Bernander focused on brittle failure and concluded that the following conditions are particularly important for the strength parameters:

- the in-situ stress state formed by the evolution of the geological features,
- the time-dependent strain involving deformation-softening and redistribution of local

---

\* Corresponding author, email: drawrite.se@gmail.com

<sup>1</sup>Luleå University of Technology, Sweden

<sup>2</sup>East China University of Technology, Nanchang, Jiangxi, China.

- high stresses,
- the loss of shear resistance in over-consolidated clay,
  - progressive failure.

Conventionally, one uses three measures of the shear strength of clay exposed to deviator stresses:

- peak strength recorded in the course of shear straining,
- residual strength representing the shear resistance at large strain,
- remoulded strength representing the strength after intense mechanical agitation.

In conventional slope stability analysis one takes the sliding clay mass as rigid and homogeneous (Figure 1) and characterized by a uniform peak strength, while for stability analyses assuming progressive and retrogressive slope failure one takes the degree of shear strain and thereby the strain-controlled shear resistance into consideration. This case was originally assumed by Fellenius in [2] and used until presently in cases where the virgin undrained shear strength, determined by fall-cone or vane-bore testing, indicates largely constant strength with increasing depth in the clay.

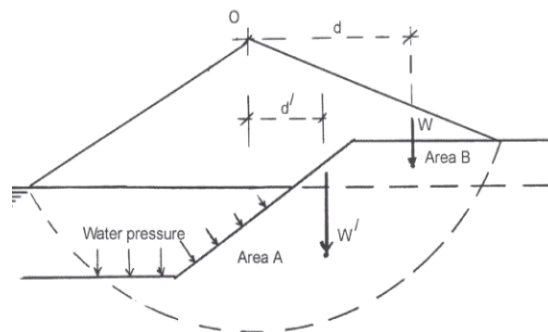


Figure 1: Assumed circular cylindrical shape of sliding clay mass assuming ideal-plastic failure analysis, disregarding from the impact of internal strain on the stress conditions within the rigid mass [2]

Paying attention to the fact that a clay mass has varying shear strength caused an improved calculation model used by Terzaghi, Taylor, Janbu and many others [3,4,5], implying that the effective pressure on the presumed slip surface determines the shear strength in  $c/\phi$  analyses, i.e. assuming that the clay has cohesion and internal friction (Figure 2). This improved basis for calculating slope stability has been accepted and used since the seventies.

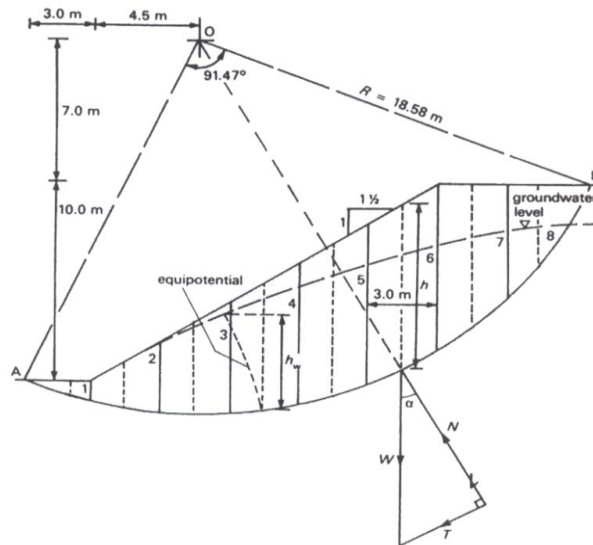


Figure 2: Example of division of a potentially unstable clay mass into lamellae for calculation of turning moments for a trial slip geometry case [5]. For the effective parameters  $c'=10$  kPa,  $\phi=28^\circ$ , and unit weight  $1800$  kg/m<sup>3</sup>, one gets  $F=1.35$

The stress distribution within the potentially sliding clay mass in Figure 2 is not uniform. It is determined by the effective normal pressure along the assumed slip plane but designers commonly pay no attention to the impact of shear strain. It is larger where the degree of strength mobilization is highest, i.e. at the toe and crown, and smaller where the available shear strength has been utilized to a lower degree, commonly in the central part of the slip plane. This means that the shear stress along the slip plane may correspond to the residual strength at the lowermost and uppermost part of the slip plane, while the shear stress may represent the peak strength in the central part of the slip plane. This assumption is reasonably correct for circular cylindrical slip surfaces but not for the common, more or less ellipsoidal shape that seems to be more common in nature. For such cases the stress situation and thereby the strain pattern within the clay mass play a role also for the shear stress distribution along the slip plane.

Bernander [1] showed that the kinetics of failing long slopes in fact govern the movements of and within them, ultimately generating passive soil pressure at the toe and active soil pressure at the crown at progressive failure. The different parts of a clay mass about to slide have undergone successive stress transition from one of maximum mobilized shear resistance to one of somewhat reduced resistance and further to one representing the residual strength, which is not the same as the remoulded shear strength. The matter is in fact very complex since those parts where large reduction of the shear resistance has taken place, generated by large strain, may undergo stiffening if the porewater pressure raised by the shearing can disseminate. The clay thereby becomes overconsolidated, using common terminology, with the higher shear resistance serving to anchor the potentially sliding mass. With time these strengthened parts undergo the same process over again, i.e. successive reduction of the shear strength due to overstressing and stress transfer to less strongly loaded parts etc, ultimately tending to give a uniform shear resistance. If it is not high enough slope failure takes place. Naturally, any external impact in the form of pile-driving, causing disturbance or pore

pressure rise by loading can be the triggering factor.

This macroscopic stress/strain model has its equivalent on the microstructural level as we will show in the present paper. We will take a practical example, the Lindö Canal, the waterway from the Baltic Sea to the city harbour in Norrköping on the Swedish eastcoast, as basis of the presentation and discussion [6].

## **2 An Example of Theoretically Unstable but still Stable Clay Slopes: The Lindö Canal**

### **2.1 Scope**

The need for a safer and deeper entrance for bigger ships to reach the city of Norrköping, some 200 km south of Stockholm, led to the decision to dredge a nearly 10 m deep and 50 m wide canal with nearly 3 km length through a typical south-Swedish landscape in the end of the fifties. The design was made by the Swedish Geotechnical Institute in the mid-fifties applying the common way of calculating the slope stability of normally consolidated illitic clay (cf. Figure 1). The channel was completed and came in use 1960, 55 years ago, making it possible for tankers with up to 16000 t deadweight to enter the harbour of the city of Norrköping from the Baltic Sea. The construction required blasting of rock with the clay to be removed still present over the rock. The blasting technique, the “Lindö method” developed by the construction company Skånska Cementgjuteriet (nowadays “Skanska”) [6], was found to give no reduction in shear strength of the remaining clay slopes after dredging. The canal has been stable from start.

At the time of design of the channel the impact of time and strain on slope stability was not considered by the geotechnical society but came in focus a few decades later and led to the development of microstructural modeling that, together with the use of rate process theory, gave a basis of more scientific treatment of slope stability involving creep processes that will be discussed and assessed here.

### **2.2 Geological and Geotechnical cConditions**

#### **2.2.1 Characterization**

The Händelö peninsula to the east of the town Norrköping belongs to the large sediment area in the inner part of the Bråviken estuary and has the typical character of glacial clay covered by postglacial clay that is at least partly eroded and redeposited glacial clay. It is hence more fine-grained than the glacial clay and free from carbonates. The clays were deposited in brackish water and have a high total content of soluble salt, i.e. 2.9 to 8.2 g/l [6]. pH is in the interval of 7.1 to 7.7. The uppermost 1.5 m, making up a dry crust, is somewhat organic with an ignition loss of 5.2 % of the dry weight while the rest has 2.8 to 3.5 % loss. The groundwater level is about 1 m below the ground surface.

The density, content of minus 2  $\mu$ m particles, consistency, Skempton’s activity, as functions of depth are given by Table 1. The lab investigations were made by the Swedish Geotechnical Institute. The water content exceeded the liquid limit for the lowest depth interval, which, together with the fact that the clay particles are significantly more oblong than in the rest of the profile, can explain the higher sensitivity [7]. Mineral analyses showed XRD reflections at 3.3, 7.0, 9.9 and 14.5 Å for all the profile, and one at 4.4 Å for

the 8 m sample. This led to the conclusion that illite (hydrous mica) was the dominant mineral and that there were small amounts of quartz and mixed-layer illite/smectite minerals. This composition fits the Skempton activity number. The 14.5 Å peak in the clay from 8 m depth probably indicates the presence of vermiculite.

Table 1: Geotechnical data of the clays in the Lindö canal area (After SGI protocols, [6] and [7])

Depth, m	Density kg/m <sup>3</sup>	Clay fraction	Water content weight %	w <sub>p</sub>	w <sub>L</sub>	IP	Activity	Shear strength <sup>1)</sup> , kPa	Sensitivity
1.8-2.0	1470-1550	85-88	77-100	27-29	97-	60-70	0.7	10.8-16.5	7.2-7.4
4.0-4.4	1430-1610	75-77	64-95	22-31	63-67	39	0.5	11.2-15.0	7.5-7.6
8.0-8.3	1560-1600	45-49	68-76	29-30	57-61	30	0.6	14.1-16.1	8.7-10.1

1) Undrained shear strength; average of cone, uniaxial compression, and vane boring tests.

The samples for cone and compression tests were taken by the best available core sampler SGI-IV for obtaining largely undisturbed samples. In the Lindö case this was supported by the agreement between vane borings and cone penetration tests. Below about 6 m depth the glacial clay contained very fine silt layers.

## 2.2.2 Design principles

The principle of SGI's slope stability analyses for determining the safety factor  $F$  was commonly adopted 50 years ago and is indicated in Fig.1, i.e. to calculate the ratio of the rotational resisting moment provided by undrained shear strength ( $c_u$ ) and the driving moment caused by the self-weight of the mass above the water level and of the submerged mass with unit weight ( $\rho_{sat} - \rho_{water}$ ). Taking the radius of the cylindrical slip surface as  $R$ , and  $\theta$  as the angle between the two radii defined in Fig.1, and assuming the water level to be constant, the factor of safety against slope failure was defined as:

$$F = c_u R^2 \theta (\pi/180) / [(Wxd) + (W'xd')](1)$$

As commonly observed, the shear resistance increases with depth meaning that failure of this type will not reach down more than to a certain depth and for potential slip surfaces reaching to the toe of the slope, the factor of safety factor can be 2-3 times higher for a slope angle of 20-30° [4,5]. In modern time the more sophisticated way of calculating the factor of safety is indicated in Figure 2. It implies dissection of the potentially unstable soil mass into vertical lamellae and the assumption of force equilibrium for each lamella in the direction of potential slip. The concept requires use of effective stresses [4,5] and the effective parameters  $c'$  and  $\phi'$  for cohesion and internal friction. This method implies that the shear strength at a potential slip surface has a fixed value that can be determined by in-situ vane testing or laboratory tests using the cone penetration method of undisturbed samples for checking the stability of old slopes, and by running drained shear box or triaxial tests for each segment of the assumed slip surface for predicting the long-term stability of slopes to be excavated. Naturally, the unloading of a clay slope by dredging causes a drop

in effective stress and therefore a successive drop in safety, which was not explicitly considered in applied soil mechanics until the effective stress concept came in general use for slope stability calculations. The branch did not consider the role of time and strain in estimating the stability of the slopes, including the Lindö Canal, following praxis at that time and even today. This has been the main criticism forwarded by Bernander [1], in his description of strain-dependent evolution of slope failure and given statement that several old slopes with a calculated safety factor of 1.1 or less have been stable for many thousands of years.

### 2.2.3 Design principles

The earliest attempt to predict the slope stability of the Lindö Canal was made by the Swedish Geotechnical Institute (SGI) using the simple method illustrated by Fig.1, which was also used for the detailed design work made in years 1956-1958 and in a complementary study in 1975. SGI's investigations were based on the assumed slope inclination 1:2 and gave a safety factor of 1.3. The relatively small spacing of the rock sections, illustrated in Fig. 3, suggested that possible circular slip surfaces would in fact be spherical but for large parts of the channel the most plausible shape would still be circular-cylindrical. The intervals of 1300 to 1400, 1675 to 2000 m, and 2300 to 2400 m are without impact of rock on the stability of the slopes.

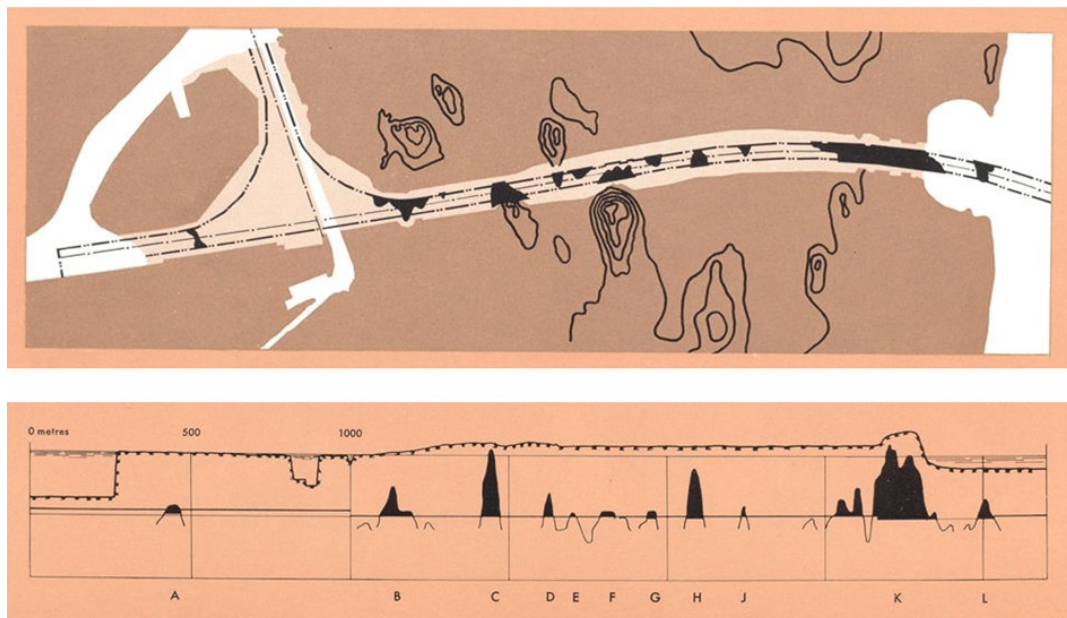


Figure 3: Overview (upper) and longitudinal section of the Lindö Canal with the presence of rock within the canal section indicated in black. To the left in the plan view: The harbour basin of Norrköping town and to the right: The Bråviken estuary [6]

### 2.2.4 Updated design of the Lindö Canal

In years 1957-1959 a comprehensive analysis of the stability of the entire canal was made based on the original undrained strength data and it showed that for 9.7 m water depth and 45 m bottom width and an inclination of the slopes of 1:2 stability would not be provided

where the ground surface was higher than 1.5 m over the average water level +/- 0. This led to adjustment of the slope profile by excavating the soil to level -1.0 within a distance of 21 m from the slope, thereby creating “banquettes” (Figure 4). This design was based on complementary determinations of the undrained shear strength that was concluded to be 11 kPa from 7 to 12 m below the ground level, and 9 kPa at smaller depths than 7 m. Plane slip surfaces were also examined and found to give lower safety factors than 1.3 for distances of the loaded area from the “banquettes” smaller than 30 m. This criterion was therefore included in the design.

Parameter analysis was not made in the design work but the impact of fluctuation of the water level and the disturbance by blasting of the clay, where underlying rock had been disintegrated, were taken into consideration. According to the Swedish Meteorological and Hydrological Institute the lowest water level in periods of at least 3 consecutive days has been -0.80 m from the construction about 50 years ago to present time. Considering this the safety factor is now concluded to have been 1.1-1.2 for considerable parts of the channel in the last 50 years. This low actual factor raises the question of whether shear-generated creep can play a role for the long-term stability and this matter was considered in some detail as described here.

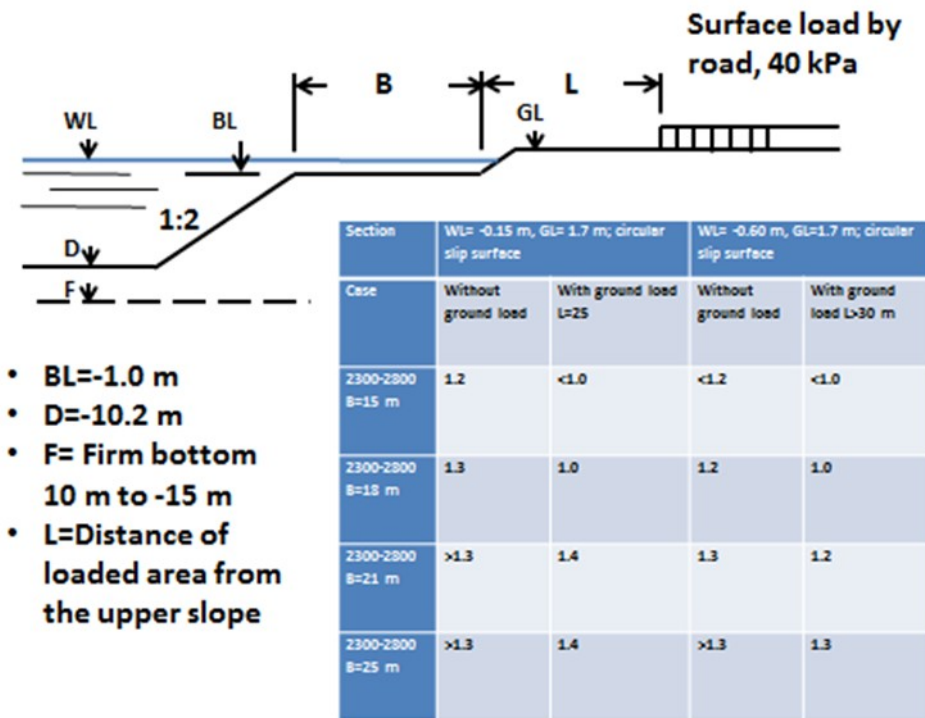


Figure 4: Summary of calculated factors of stability. The right column represents the stability conditions for the selected design with B=20 m, L=30 m and slope inclination 1:2.

### 3 Creep affecting Slope Stability

#### 3.1 Impact of Shear Strain

The actual shape of the curved potential slip plane in Fig.1 must be adapted to the geometry and strength of the various soil layers, implying that the shear resistance mobilized in each individual part of the assumed slip plane or zone, depends on the strain that it undergoes. A critical state can thence be reached locally while the overall stability is still maintained. Complete and large-scale failure occurs when the maximum shear resistance has been fully mobilized. In the old days little or no respect was paid to the time dependence of the successive weakening of freshly cut clay slopes while modern rate process theory offers ways of including the impact of both strain and time. One can therefore now define the conditions for successive changes in stability and explain why slopes excavated in normally consolidated clay can be stable for very long periods of time even if the calculated safety factor  $F$  derived from simple  $c$ -analyses is only slightly higher than unity. The role of time-dependent shear strain (creep) has thereby been found to be stabilizing in contrast to the common belief that it is destabilizing.

#### 3.2 Role of Creep Strain

The literature described a number of investigations dealing with the role of strain rate on the ability of soft illitic clay to resist shear stresses. They include testing of the effect of imposed strain rate on the undrained strength, the creep behaviour at “controlled rate of shearing” (CRS), and determination of creep strain of all sorts of soft clays under different conditions. A general observation is the large difference in rupture life and increase or decrease of the unconfined compressive strength by creep strain. An often cited report was published by Campanella and Vaid in 1974 dealing with triaxial and plane strain testing, ending with the conclusion that effective stress failure in creep rupture is governed by the same linear failure envelope that is obtained at ordinary shear testing [8]. In 1993 Kuhn and Mitchell reported that clays exhibit viscous creep behaviour and proposed a mechanism for both viscous and frictional interparticle sliding based on rate process theory [9]. Their conclusion agreed with that of most other investigators’ that the creep rate increases with greater applied stress and that illitic clays exhibit creep rupture at high stress levels. They did, however, not provide any conceptual model of the shear/relaxation mechanisms on the microstructural level. We will propose such a model in the present paper and explain how these mechanisms can cause overconsolidation that explains why clay slopes can stay stable for very long period of time but fail by sudden disturbance or overloading.

Figure 5 shows the recorded creep strain of a marine illitic clay from Bäckebol near Gothenburg, Sweden, with a density at saturation of  $1500 \text{ kg/m}^3$  and an undrained shear strength ( $\tau_{fi}$ ) of 23 kPa. The curves represent the recorded strain under shear stresses representing 70%, 85%, and 90% of the conventionally determined undrained shear strength. The clay had a water content of 93 % and a liquid limit of 94 %. The sensitivity, expressed as the ratio of the undisturbed and remoulded shear strengths, was 26. For the lowest shear stress the creep attenuated according to a log-time relationship, while for the intermediate stress the strain rate tended to become constant hence approaching the state of secondary creep that is believed to be associated with comprehensive microstructural reorganization. The highest stress gave quick failure. For this clay the rate of strain 1



minute after onset of creep was about  $E-3 \text{ s}^{-1}$  and about  $E-5 \text{ s}^{-1}$  after 30 minutes, suggesting that the shear stress has to be in the interval 70-85% of the undrained shear strength for avoiding ultimate failure. This implies that the safety factor in practice should be higher than about 1.4, which is, in principle, in agreement with common recommendations for safe slope design.

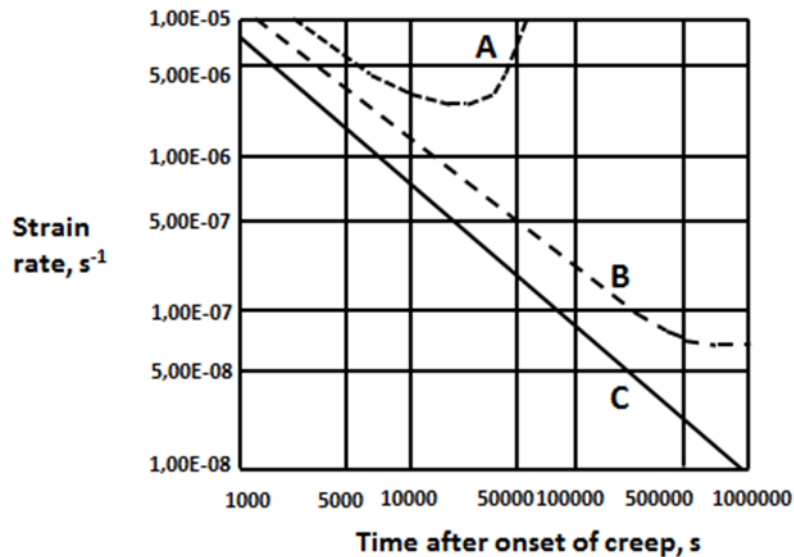


Figure 5: Recorded creep strain of a marine illitic clay from Bäckebol near Gothenburg with a density at saturation of  $1500 \text{ kg/m}^3$  and an undrained shear strength ( $\sigma_{fi}$ ) of 23 kPa (Geot. Div. Chalmers Techn. Univ.) A, B and C represent 90%, 85%, and 70% of the conventionally determined undrained shear strength

Further examples of recorded creep strain of marine and fresh-water clays and organic clay, tested by uniaxial and triaxial loading, are shown in Fig. 6, which illustrates that inorganic illitic clay loaded to 50-70% of the conventionally determined undrained shear strength in principle follow the log-time. In this graph “loading” is the uniaxial pressure in percent percentage of the conventionally determined unconfined compressive strength of the respective clay. Loading to <50% hence means that the factor of safety was equal to or lower than 1.5 while loading to 75% corresponds to a safety factor of 1.33. We see from the D-curve in Fig. 6 that the evolution of creep for this safety factor is of the type represented by Curve B in Fig. 6, hence tending to represent “second-order creep” and ultimate failure. For soft organic clays even the higher safety factor of 1.5 can give the same trend (Curve E), while dense organic-rich clay (Curve F) can behave as inorganic clays but with somewhat higher creep rates. For clays with more than about 1 weight percent of humic substances this component tends to determine the strain and strain rate. It is interesting to see that fresh-water clays behave in principle like marine clays and that all the clays, except the organic ones, behaved similarly. For low and moderate shear stresses creep attenuates according approximately to a log-time relationship [10].

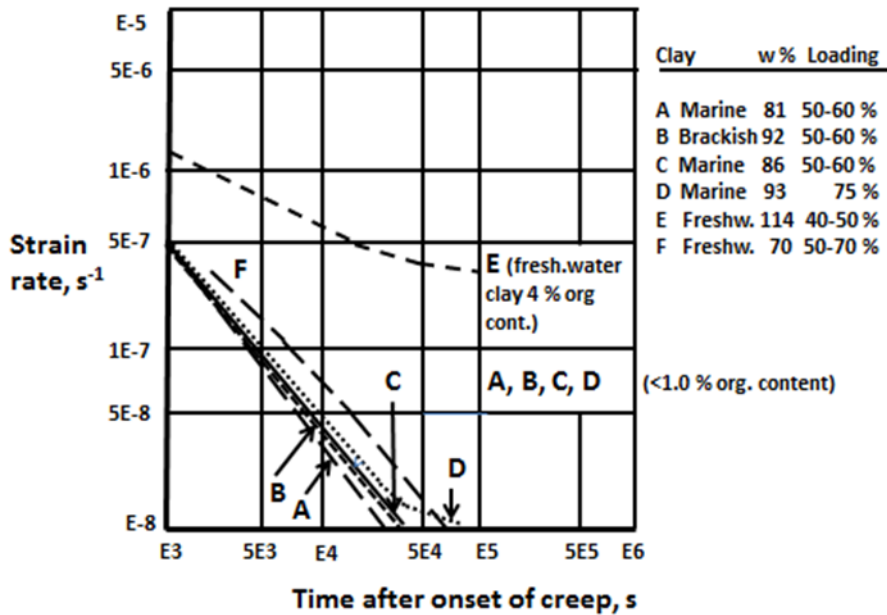


Figure 6: Creep curves of Quaternary illite-dominated clays\* under uniaxial compression. The actual loading rates are in percent of the respective failure load

### 3.3 Creep Pate Modelling

The variation in strength over cross sections or volumes suggests application of statistical mechanics for working out conceptual models to be converted to get theoretical forms. This has been tried by various investigators but commonly without considering the actual spectrum of bond strength, or rather, the spectrum of energy barriers (Figure 7). Following the principle introduced by Feltham and Pusch [11, 12, 13] taking various scale-dependent creep-producing structural features into consideration in formulating creep models for the microstructural scale:

- The application of a deviator stress exceeding the one existing previously in the clay mass causes elastic strain on the microscale and initiates slip, i.e. local plastization, in the form of translatory shear displacement at overstressed particle contacts in clay,
- Redistribution of stresses is facilitated by slip by which higher local stresses are generated where previously they were low, the associated strain enhancing the bulk creep rate,
- The bulk strain induces local displacements such that stronger units make contact and help to strengthen the structure. This involves microdilatancy and mechanical interlocking, which are the major “healing” processes by which the creep rate is retarded. In principle creep is produced by the continuation of the slip process involving breakage of low energy barriers and activation of high-energy barriers,

\*A, B, C, D represent marine clays from Lilla Edet, southwest Sweden; E, F fresh-water clays from Skå Edeby, Stockholm area; G Köping city 150 km west of Stockholm.

- which successively will dominate,
- As long as the deforming microstructure is coherent, which requires that the bulk stress is not critically high, dominance of high-energy barriers means that the material becomes charged with high energy, making it brittle. Triggering of failure by increasing the bulk stress will give instantaneous breakage.
  - The interparticle bonds in clay range from very low London/van der Waals and hydrogen bonds to high primary chemical bonds, i.e. from a fraction of 1 electron volt to energies higher than 25 kcal/mole [14]. Mechanical friction between contacting asperities of silt and sand grains, aided by dilation, generates high shear resistance and represents strong bonds.



Figure 7: High-voltage transmission electron image of specimen of natural illite clay saturated with water [14]. Various interparticle bond types can be imagined in the coherent clay specimen: Primary chemical bonds, Coulomb electrostatic couplings, shared between sorbed cations, and hydrogen bonds *en masse*

The net effect of the various mechanisms is controlled by the magnitude of the bulk deviator stress and strain, as well as by the boundary conditions, which can put a limit to the strain. The entire creep process in clay can be understood as thermally assisted passages over energy barriers driven by external bulk stresses.

This conceptual microstructural creep model can be expressed in mathematical form by considering:

- The structural heterogeneity and bond strength variation expressed by a spectrum in bond strength or activation energy,
- That each clay element contains a certain number of slip units (patches of atoms) in a given interval of the activation energy spectrum at any particular time after the onset of creep,
- That, in the course of the creep, new slip units are created at the lower end of the energy spectrum while the high energy end is an “absorbing barrier”, representing a “blue-shift” of the spectrum,
- That jumps on the atomic or molecular scale bring a slip unit up or down against a

barrier by a certain amount, higher or lower than the previous one. Applying thermodynamics the number of potential slip units per unit volume held up at barriers of a certain height can be defined by use of the Arrhenius rate equation  $v(u)=v_D \exp(-u/kT)$ , introducing an averaged atomic vibrational frequency  $v_D$  and using Boltzmann's constant and the absolute temperature [12],

- Introduction of a relevant number of energy barriers of certain height and energy interval between successive jumps of a unit, making the entire process stochastic. The change in activation energy in the course of evolution of strain means that the number of slip units is determined by the outflux from any energy level into the adjacent, higher energy interval and by a simultaneous inflow into the interval from the lower part of the barrier spectrum,
- That when a slip has taken place, meaning that a barrier has been overcome, a contribution to the bulk shear strain has been made by the associated extension of the local slip-patch. The next barrier to be encountered by the same spreading slip unit will be either higher or lower by the same average amount of energy.

For low shear stresses, allowing for “uphill” rather than “downhill” jumps and assuming that each transition of a slip unit between consecutive barriers gives the same contribution to the bulk strain one gets the bulk shear strain rate as in Eq.(2) with  $t < t_o$  as boundary condition:

$$d\gamma/dt=B(1-t/t_o) \quad (2)$$

The coefficient B and the value of  $t_o$  depend on the deviator stress, temperature and structural details of the slip process. The creep strain can be expressed as in Eq. (3), meaning that the creep starts off linearly with time and then dies out, hence corresponding to “primary” creep.

$$\gamma=at -\beta t^2, (t < a/2\beta) \quad (3)$$

where  $a$  and  $b$  are constants.

For higher bulk deviator stresses, the strain on the microstructural level yields some irreversible changes associated with local breakdown and reorganization of whole particles. Still, there is repair by inflow of new low-energy barriers parallel to the strain retardation caused by the successively increased number of slip units that meet higher energy barriers as illustrated by the “blue-shift” of the energy barrier spectrum exemplified in Fig. 8. This type of creep can go on forever without approaching failure. Feltham [11] demonstrated that for thermodynamically appropriately defined limits of the u-spectrum the strain rate appertaining to logarithmic creep takes the form of Eq. (4):

$$d\gamma/dt=BT\tau/(t+t_o) \quad (4)$$

where  $B$  is a function of the shear stress  $\tau$ .  $t_o$  is a constant of integration which leads to a creep relation closely representing the commonly observed logarithmic type implying that the creep strain is proportional to  $\log(t+t_o)$ .

The detailed microstructural process involves early triggering of low barriers associated with activation of new slip units at the lower end of the barrier spectrum, which represents the “generating barrier” end, while the upper is “absorbing”. The energy spectrum hence changes in the course of the creep as illustrated by Figure 8, which represents the case of

initially uniform distribution of barriers in the assumed interval 0.1-0.9 eV. The graph shows the calculated successive change in the number of barriers of different activation energies as a function of time. At the end of the creep period (stage 5) the number of very low barriers has dropped from the initially assumed number 100 to 1, while those representing 0.5 eV have increased from 100 to about 400 [9]. If the shear stress is kept constant the energy spectrum moves from lower to higher levels in the course of the mobilization of stronger barriers and the system becomes dominated by strong interparticle bonds.

The practical meaning of all this is that the large majority of contacting clay aggregates are “hung up” in old natural clay slopes and that they do not exhibit significant creep. High stresses prevail at these contacts but rather small external impact, like pile-driving or road construction close to the crown of the slope can trigger failure.

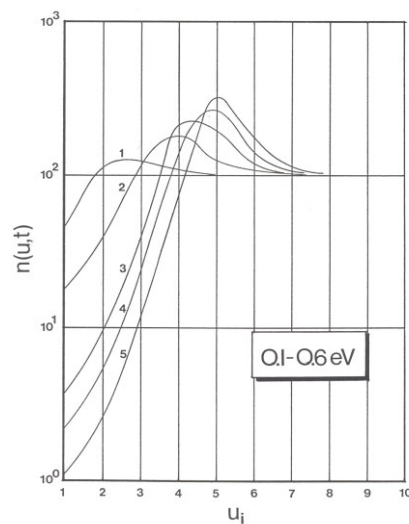


Figure 8: Successive change in distribution of energy barriers in the course of transient creep. 1, 2, 3 etc denote time stages and  $n(u,t)$  the fraction of barriers of energy level  $u_i$ . The initial number of barriers is 1000 [13]

The significance of  $t_o$  is understood by considering that in the course of applying a deviatoric stress, at the onset of the creep test, the deviator rises from zero to its nominal, final value. A  $u$ -distribution exists at  $t=0$ , i.e., immediately after full load is reached, which may be regarded as equivalent to one which would have evolved in the material initially free from slip units, creep had taken place for a time  $t_o$  before loading. This behaviour was shown by the rather soft freshwater clay represented by Curve F in Figure 4. Negative  $t_o$  has been found for significantly cemented clay (Figure 9).

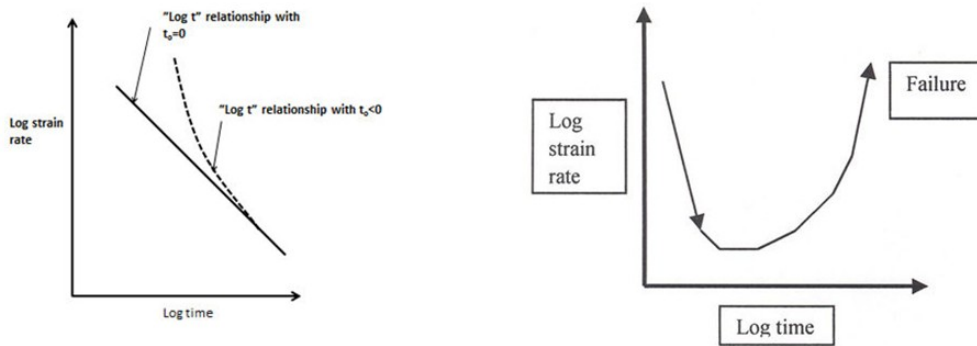


Figure 9: Generalization of creep curves of log time type [10]

A simplified interpretation of the performance of the model is that at the lower end of the energy spectrum new energy barriers are generated and at the other end higher energy barriers accumulate while weak bonds are broken. This leads to a state of successively increased strength and stiffness in conjunction with stress transfer from overloaded parts of the microstructural networks to stronger parts. The higher barriers become located in more rigid and stronger microstructural components.

This model implies, for moderate deviator stresses that allow for microstructural recovery, that the creep strain is as in the left drawing of Figure 9. If there is successive retardation of the creep rate according to the logarithmic time law, failure is not expected even after very long periods of time provided that the particle network remains coherent, which in turn implies that the total strain is not too large. Further increase in deviator stress leads to “secondary creep” - the horizontal part of the curve in the right drawing of Figure 9 - where the strain rate tends to be constant and the strain proportional to time. The then high creep rate does not allow for microstructural self-repair and the strain eventually becomes critically large, leading to failure: comprehensive slip changes the structure without allowing reorganization. For smectite clay, shear-induced formation of slip units consisting of dispersed stacks of  $10\text{\AA}$  lamellae, is much more comprehensive than in illitic and kaolinite-rich clays. The successive increase in the number of slip units in fact implies an important self-sealing ability that causes attenuation of the creep rate even for high shear stresses (Figure 10). Smectite-rich clays in fact behave as viscous fluids at large strain but they eventually fail by loss of coherence at large strain. One finds, from the creep diagrams in Fig.7 that the behaviour of the smectite clay for the low shear stress 6 kPa, i.e. about 25 % of the shear strength 23 kPa, represents primary creep of Eq. (3) type.

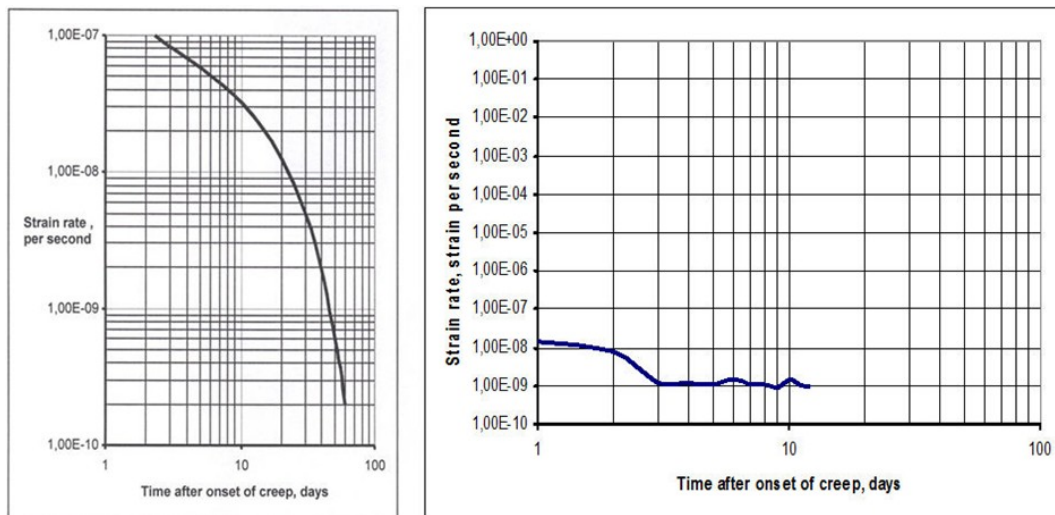


Figure 10: Creep of smectite-rich clay (MX-80) with a density at saturation with distilled water of  $1500 \text{ kg/m}^3$ . Left: steeply declining curve representing primary creep obtained for the shear stress 6 kPa. Right: nearly constant strain rate representing secondary creep after increasing the shear stress to 23 kPa [15]

A couple of decades after completing the construction it was decided to measure the creep rate of the slopes in four sections. A theodolite was mounted in specially constructed wells with accurately measured positions, from the bottom of which flexible tubes were inserted in vertical boreholes for measuring horizontal strain. The tubes were anchored in moraine at 10 m depth. Recording of the horizontal displacement of their vertical axes were made in December 1962 and January 1963, from which one concluded that creep strain in this period occurred only in one section (1675) where it amounted to about 3 mm at 1 m depth, 6 mm at 3 m, 8 mm at 4 m, and 4 mm at 7 m depth [6]. The accuracy of the measurements was limited because of temperature impact on the reference points and the only safe conclusion was that the shear displacements were confined to 3 to 5 m depth of the slope. This agrees with the location of the zone with highest shear stresses.

### 3.4 Application to Slope Stability

Movements and failure of cuts and natural slopes have been reported and discussed by Leroueil and Tavernas [16,17] who defined and described different stages of slope movements: pre-failure, failure, post-failure and reactivation (cf. also [18] and [19]). They put emphasis on the origin and function of brittleness of soils and their practical importance for the progressive failure developing at the pre-failure stage. Precipitation of cementing substances and changes in groundwater chemistry affecting chemical interparticle bonds by cation exchange are possible reasons for brittleness and overconsolidation. Such impact is not believed to have affected the clay slopes of the Lindö Canal since environmental control of the water quality in it and in the inner part of the Bråviken estuary, where fishing is comprehensive, have not indicated any contamination or change in salinity. Therefore, creep-induced stiffening as described here may well be the main reason for the rather unexpected slope stability. It would cause

strengthening of the clay but also increased sensitivity to disturbance by pile-driving or earth shocks.

#### 4 Discussion and Conclusions

Load-generated shear stresses in normally consolidated illitic clay by loading, or by unloading caused by slope excavation, creates a local stress state that can lead to failure if the mobilized shear stress exceeds a certain critical value, which is believed to be on the order of 2/3 of the conventionally determined bulk strength [10]. This corresponds roughly to a safety factor of 1.3-1.4. For lower stresses the bulk strain corresponds to the integrated very small slips leading to “primary creep” with attenuating strain rate. For critically high stresses the rate of mobilization of new particle bonds is too low to maintain microstructural continuity and “secondary” creep, ultimately leading to bulk failure, is reached. The mechanisms leading to shear strain in a homogeneous clay mass are complex, especially if cementation has taken place and cause brittleness. This is conventionally taken to be due to precipitated cementing agents like carbonates and iron complexes but can also be caused by microstructural strain leading to dominance of high energy barriers to interparticle displacement as explained in this paper.

The reason why the Lindö Canal and several natural long slopes with similar low safety factors on the Swedish west-coast are stable can be explained by application of the proposed theory, which defines the conditions for retarded and accelerated creep strain. It explains the stability by considering the strain mechanisms on a microstructural scale: sufficiently slow deformation mobilizes higher energy barriers to particle slip on the expense of lower ones. This suggests that stable conditions can prevail for any period of time even for low safety factor values provided that failure is not triggered by disturbance in the form of externally generated porewater overpressure, loading, or vibrational disturbance. It is implicit that soft collapsible clay undergoing long-term creep, become more brittle. An overall conclusion from this study is that simple slope analyses using the undrained shear strength can be satisfactory as long as the shear stress does not exceed the undrained shear strength. The following major conclusions are summarized:

- slopes excavated in normally consolidated illitic clay can be stable for a very long time even for calculated safety factors as low as unity based on the undrained shear strength, provided that weakening is not triggered by disturbance in the form of pile driving, road construction or excavation close to them. The Lindö Canal is believed to be a representative of such conditions,
- excavation of a slope in normally consolidated illitic clay generates bulk shear stresses causing irreversible changes in the form of local microstructural breakdown and reorganization. This mobilizes inflow of new low-energy barriers, which increases the number of slip units that become held up by meeting higher energy barriers. If the healing processes at creep strain outweigh the damaging ones this type of creep is of log-time type and can go on forever without approaching bulk failure. For higher bulk stresses the rate of mobilizing low-energy barriers can be insufficient and the bulk strain rate can then accelerate and cause failure. For very low bulk stresses there is time for microstructural repair by mobilizing higher energy barriers, which leads to rapid reduction of the strain rate that ultimately dies off,



- for clays undergoing creep in very long time the interparticle bonds carry successively higher stresses, which makes it successively more sensitive to disturbances and potentially unstable and brittle. The Lindö Canal may represent such a case.

**ACKNOWLEDGEMENTS:** The authors like to express their sincere gratitude to the Technical Manager of Norrköping Hamn och Stuveri AB, Raymond Axelsson, for his engagement and assistance in finding relevant documents concerning the design, construction and observations of the Lindö Canal. They are also grateful to Prof. Emeritus Raymond Yong, Canada, for his valuable comments. Thanks are also due to our doctoral student Qi Jia at the Geotechnical Division, Luleå University of Technology, Luleå, Sweden for preparing the paper.

## References

- [1] Bernander, S., Progressive landslides in long natural slopes. Doct. Thesis, Luleå University of Technology (ISBN: 978-91-7439-283-8; ISSN: 1402-1544), Luleå, Sweden, 2011.
- [2] Fellenius, W., Quay and soil failure. *Teknisk Tidskrift* (Sweden), Vol.2, (1918), pp.17-19.
- [3] Terzaghi, K. & Peck, R.B., *Soil Mechanics in Engineering Practice*. John Wiley & Sons, New York, 1948.
- [4] Taylor, T.W., *Fundamentals of Soil Mechanics*. John Wiley, New York, pp. 345-392, 1948.
- [5] Janbu, N., State-of-the-Art Report: Slopes and excavations. Proc. 9th ICSMFE, Tokyo, 1977.
- [6] Internal reports and calculations conc. The Lindö Canal. Norrköping Hamn och Stuveri AB. Norrköping Community, Sweden.
- [7] Pusch, R., *Clay Particles*. Dr Thesis, Royal Technical Institute (KTH), Stockholm, 1962
- [8] Campanella, R.G. & Vaid, Y.P., Triaxial and plain creep rupture of an undisturbed clay. *Can. Geot. J.*, Vol.11, (1974), pp.1-10.
- [9] Kuhn M. & Mitchell, J., New perspectives on soil creep. *J. Geotech. Engrg*, Vol. 119(3), (1993), pp.507-524.
- [10] Pusch, R., & Yong, R.N., *Microstructure of smectite clays and engineering performance*. Taylor & Francis, London & New York, (ISBN: 0-415-36863-4), 2006.
- [11] Feltham, P., A stochastic model of creep. *Phys. Stat. Solidi*, Vol.30 (1968), pp.135-146.
- [12] Pusch, R. & Feltham, P., A stochastic model of the creep of soils. *Géotechnique*, Vol.30, No.4, (1980), pp. 497-506.
- [13] Pusch, R., & Feltham, P., Computer simulation of creep of clay. *J. of the Geotechnical Engineering Division, ASCE*, Vol. 107, No. GT1. (1981), pp. 94-104.
- [14] Pusch, R., A technique for investigation of clay microstructure. *Journal de Microscopie*, Vol.6, (1967), pp.963-986.
- [15] Pusch, R., *Geological storage of radioactive waste*. Springer Verlag (ISBN: 978-3-540-77332-0), 2008.

- [16] Tavernas, S. & Leroueil, Creep and failure of slopes in clay. *Can. Geot. J.*, Vol.18 (1), (1981), pp.106-120.
- [17] Leroueil, S., 39th Rankine Lecture: Natural slopes and cuts: movements and failure mechanisms. *Géotechnique*, Vol.51,(2001), pp.197-243.
- [18] Chun-Man Cheng & Jian-Hua Yin,. CRS testing. *Marine Georesources and Geotechnology*, Vol.25, (2005), pp.61-92.
- [19] Federico, A., Popescu. M., Elia, G., Fidelibus, C., Internò, G., Murianni, A., Prediction of time to slope failure: a general framework. *Environmental Earth Sciences*, Vol.66 (1), (2012), pp.245-256.